Stress State for Pipes Made of a Concrete and Fiber Glass when Change the Angle of the Reinforcing

Tymor Abed Alsattar Sediq

Technical Education, Mosul Technical Institute, Mosul, Iraq

(tymorabed@yahoo.com)

Abstract- The purpose of this paper was to overcome economic issue, which is one of the major barriers of the use of FRP in civil engineering. The analysis of the methods of definition of elastic characteristics of separate layers reinforced by high-module fibers on the macro level is given. In the case, when the composite itself represents a set of layers with different directions of reinforce, the technique of the given elastic characteristics definition and component of matrixes of rigidity of all layers' package as a whole is offered.

Keywords- *fiber glass; concrete; pipes; stress state; composite materials; reinforcing.*

I. INTRODUCTION

Composite is defined as a mechanically separable combination of two or more component materials, different at the molecular level, mixed purposefully in order to obtain a new material with optimal properties, different than the properties of the components (definition based on [1 -3]).

Composite materials have been used in construction for centuries. One of the first was the use of straw as reinforcement in mud and clay bricks by the ancient Egyptians [4]. The combination of reinforcing steel and concrete has been the basis for a number of structural systems used for construction for the last century. The new class of composite materials, gradually gaining acceptance from civil engineers, both for the rehabilitation of existing structures and for the construction of new facilities, are fiber Reinforced Polymer composites, primarily developed for the aerospace and defense structures.

Fiber Reinforced Polymer composites are the combination of polymeric resins, acting as matrices or binders, with strong and stiff fiber assemblies which act as the reinforcing phase [2]. The combination of the matrix phase with a reinforcing phase produces a new material system, analogous to steel reinforced concrete, although the reinforcing fractions vary considerably (i.e., reinforced concrete in general rarely contains more than 5% reinforcement, whereas in FRP composites, according to various sources [1 - 5], reinforcing volume fraction ranges from 30-70%).

Although the steel reinforcement in concrete structure is protected by concrete, aggressive environmental condition can stimulate the carbonation of concrete and the formation of hydrated ferrous oxide in steel, resulting in spalling of concrete cover. The primary cause of deterioration of concrete pipe is the corrosion of steel reinforcement. Since FRP composite exercises high corrosion resistance, it can be used to replace steel reinforcement in the forms of rebars for flexural and shear reinforcements, and tendons for prestressing or post-tensioning. FRP rebar and tendon can take the form of one dimensional or multidimensional shape, depending on type of application. There have even been some attempts to incorporate wireless sensing into infrastructure using FRP reinforcement. However, there are several challenges in using FRP rebar and tendon. One issue is the linear elastic behavior of FRP rebar when loaded to failure. This means that concrete element reinforced using FRP rebar may not have the same ductile failure of steel-reinforced element. Its lower modulus of elasticity also leads to serviceability problems, such as larger deflection and larger crack widths [2].

The aim of this paper is to present FRP composites as the new material used for the purposes of civil engineering and prepare the state of the art in pipes structures using FRP composites for structural elements as the substitution of traditional materials.

II. THEORETICAL BASES OF CALCULATION OF ELASTIC CHARACTERISTICS OF MULTILAYER MATERIALS

For orthotropic material calculated according to the elastic properties of high-modulus steel layer have the form [6]:

$$E_1^{(k)} = \psi_1^{(k)} E_B + \frac{(1 + \psi_1^{(k)})(1 + \psi_3^{(k)})}{1 - \psi_1^{(k)}} E_M;$$

$$E_2^{(K)} = \frac{(1+\psi_1^{(k)})(1+\psi_3^{(k)})}{(1-\psi_1^{(k)})(1-\psi_3^{(k)})(1-v_B^2)} E_M;$$

$$E_3^{(k)} = \psi_3^{(k)} E_B + \frac{(1+\psi_1^{(k)})(1+\psi_3^{(k)})}{(1-\psi_1^{(k)})(1-v_B^2)} E_M;$$

$$v_{12}^{(k)} = \frac{v_B(1+\psi_3^{(k)})(1+\psi_1^{(k)})}{\psi_1^{(k)}(1-\psi_3^{(k)})(1-\psi_3^{(k)})(1-v_B^2)} \cdot \frac{E_M}{E_B};$$

$$v_{13}^{(k)} = v_B\psi_3^{(k)} + (1-\psi_3^{(k)})v_B; \qquad v_{23}^{(k)} = v_B\psi_3^{(k)} + (1-\psi_3^{(k)})v_M;$$

$$G_{12}^{(k)} = \frac{(1+\psi_1^{(k)})}{(1-\psi_1^{(k)})(1+\psi_3^{(k)})} G_M; \qquad G_{23}^{(k)} = \frac{(1+\psi_3^{(k)})}{(1-\psi_3^{(k)})(1-\psi_1^{(k)})} G_M;$$

$$G_{13}^{(k)} = \frac{(1+\psi_1^{(k)})(1+\psi_1^{(k)})}{(1-\psi_1^{(k)})(1-\psi_3^{(k)})} G_M, \qquad (1)$$

Where the subscript "в" refers to the reinforcement (steel), "м" refers to the binder (concrete); $\psi_1^{(k)}, \psi_3^{(k)}$ - the relative volume content reinforcement layer in the direction of axes (1) and (3) (see Fig. 1). Shear modulus of the steel and concrete are determined by the dependencies

$$G_B = \frac{E_B}{2(1+V_B)}; \qquad G_M = \frac{E_M}{2(1+V_M)}. \qquad (2)$$

Where: $V_в, V_м$ - Poisson's ratio coefficient of reinforcement $\psi_1^{(k)}$, which characterizes the relative volume content of steel, can be determined by the formula:

$$\psi_1^{(k)} = \frac{\pi(d_B^{(k)})^2}{4h^{(k)}} i_B^{(k)}, \qquad (3)$$

Where: $h^{(k)}$ – thickness of the reinforced layer, $d_B^{(k)}$ - steel diameter; $i_B^{(\kappa)}$ – frequency of reinforcement $\psi_3^{(\kappa)}$ determined using empirical relationships and, as typically, changes in the interval $\psi_3^{(\kappa)} = (0,05 \div 0,15)\psi_1^{(\kappa)}$.

The geometry of the reinforced layer is shown in (Fig. 1.a). All quantities with index (K) refers to the K- layer shell. Elasticity relationships for an orthotropic unidirectional reinforced layer in its axis of symmetry, taking into account physical and technical constants (1) - (3) in matrix form are as follows:

$$\sigma_{(k)}{}' = a_{(k)}{}' \varepsilon_{(k)}{}' , \qquad \varepsilon_{(k)}{}' = b_{(k)}{}' \sigma_{(k)}{}' , \qquad (4)$$

$$\sigma_{(k)}{}' = [\sigma_{1'1'}^{(k)}, \sigma_{2'2'}^{(k)}, \sigma_{3'3'}^{(k)}, \sigma_{2'3'}^{(k)}, \sigma_{1'3'}^{(k)}, \sigma_{1'2''}^{(k)}]^T,$$

$$\varepsilon_{(k)}{}' = [\varepsilon_{1'1'}^{(k)z}, \varepsilon_{2'2'}^{(k)z}, \varepsilon_{3'3'}^{(k)z}, \varepsilon_{2'3'}^{(k)z}, \varepsilon_{1'3'}^{(k)z}, \varepsilon_{1'2''}^{(k)z}]^T$$

column matrix of stress and strain layer in the direction of axes of symmetry $1'$, $2'$ (Fig. 1, b);

$$a_{(k)}' = \begin{bmatrix} a_{11}^{(k)} & a_{12}^{(k)} & a_{13}^{(k)} & 0 & 0 & 0 \\ a_{21}^{(k)} & a_{22}^{(k)} & a_{23}^{(k)} & 0 & 0 & 0 \\ a_{31}^{(k)} & a_{32}^{(k)} & a_{33}^{(k)} & 0 & 0 & 0 \\ 0 & 0 & 0 & a_{44}^{(k)} & 0 & 0 \\ 0 & 0 & 0 & 0 & a_{55}^{(k)} & 0 \\ 0 & 0 & 0 & 0 & 0 & a_{66}^{(k)} \end{bmatrix}, \quad b_{(k)}' = \begin{bmatrix} b_{11}^{(k)} & b_{12}^{(k)} & b_{13}^{(k)} & 0 & 0 & 0 \\ b_{21}^{(k)} & b_{22}^{(k)} & b_{23}^{(k)} & 0 & 0 & 0 \\ b_{31}^{(k)} & b_{32}^{(k)} & b_{33}^{(k)} & 0 & 0 & 0 \\ 0 & 0 & 0 & b_{44}^{(k)} & 0 & 0 \\ 0 & 0 & 0 & 0 & b_{55}^{(k)} & 0 \\ 0 & 0 & 0 & 0 & 0 & b_{66}^{(k)} \end{bmatrix} -$$

Matrix stiffness and pliability K - rank orthotropic layer in the direction of symmetry axes $1'$, $2'$ respectively.
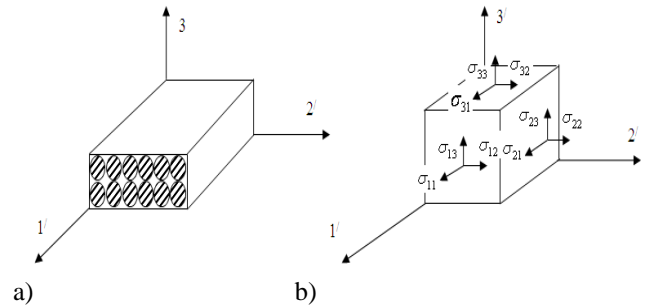
Figure 1 Unidirectional steel reinforcement scheme

Solving two systems of equations (4) with respect to stiffness $a_{ij}^{(k)}$, we can find the following relations:

$$a_{11}^{(k)} = \left[b_{22}^{(k)} b_{33}^{(k)} - \left(b_{23}^{(k)}\right)^2 \right] \Delta_{(k)}^{-1}, \qquad a_{22}^{(k)} = \left[b_{11}^{(k)} b_{33}^{(k)} - \left(b_{13}^{(k)}\right)^2 \right] \Delta_{(k)}^{-1},$$

$$a_{33}^{(k)} = \left[b_{11}^{(k)} b_{22}^{(k)} - \left(b_{12}^{(k)}\right)^2 \right] \Delta_{(k)}^{-1}, \quad a_{12}^{(k)} = \left[b_{13}^{(k)} b_{23}^{(k)} - b_{12}^{(k)} b_{33}^{(k)} \right] \Delta_{(k)}^{-1}, \quad (5)$$

$$a_{13}^{(k)} = \left[b_{12}^{(k)} b_{23}^{(k)} - b_{22}^{(k)} b_{13}^{(k)} \right] \Delta_{(k)}^{-1}, \qquad a_{23}^{(k)} = \left[b_{12}^{(k)} b_{13}^{(k)} - b_{11}^{(k)} b_{23}^{(k)} \right] \Delta_{(k)}^{-1},$$

$$\Delta_{(k)} = b_{11}^{(k)} b_{22}^{(k)} b_{33}^{(k)} + b_{12}^{(k)} b_{23}^{(k)} b_{31}^{(k)} + b_{21}^{(k)} b_{32}^{(k)} b_{13}^{(k)} - b_{13}^{(k)} b_{22}^{(k)} b_{31}^{(k)} - b_{21}^{(k)} b_{12}^{(k)} b_{33}^{(k)} - b_{11}^{(k)} b_{32}^{(k)} b_{23}^{(k)},$$

$$a_{44}^{(k)} = \frac{1}{b_{44}^{(k)}}, \qquad a_{55}^{(k)} = \frac{1}{b_{55}^{(k)}}, \qquad a_{66}^{(k)} = \frac{1}{\hat{a}_{66}^{(k)}}.$$

Compliance coefficients $b_{ij}^{(k)}$ can be written by technical constants (1):

$$b_{11}^{(k)} = \frac{1}{E_1^{(k)}}, \quad b_{12} = -\frac{v_{21}^{(k)}}{E_2^{(k)}}, \quad b_{13} = -\frac{v_{31}^{(k)}}{E_3^{(k)}}, \quad b_{21} = -\frac{v_{12}^{(k)}}{E_1^{(k)}},$$

$$b_{22}^{(k)} = \frac{1}{E_2^{(k)}}, \quad b_{23} = -\frac{v_{32}^{(k)}}{E_3^{(k)}}, \quad b_{31} = -\frac{v_{13}^{(k)}}{E_1^{(k)}}, \quad b_{32} = -\frac{v_{23}^{(k)}}{E_2^{(k)}},$$

$$b_{33}^{(k)} = \frac{1}{E_3^{(k)}}, \quad b_{44} = \frac{1}{G_{23}^{(k)}}, \quad b_{55}^{(k)} = \frac{1}{G_{13}^{(k)}}, \quad b_{66}^{(k)} = \frac{1}{G_{12}^{(k)}}$$

If the thick-walled element consists of a unidirectional reinforced layers, the axis of local coordinate systems that do not coincide with the axes of the global coordinate system, that is, for example, in cross-reinforced shells, it is possible to vary the material properties due to the angle of reinforcement

Let β - the angle between the axes of symmetry k – layer shell $\alpha_1^{(k)\beta}$, $\alpha_2^{(k)\beta}$ and the directions of coordinate lines $\alpha_1^{(k)}$, $\alpha_2^{(k)}$, т.е. corner reinforcement. It is known that in the rotated axes ($\alpha_1^{(k)\beta}$, $\alpha_2^{(k)\beta}$, z) reinforced layer has anisotropic properties and has one plane of elastic symmetry. Then becoming fair ratio of elasticity:

$$\sigma_{(k)} = a_{(k)}^{\beta} \varepsilon_{(k)}, \tag{6}$$

Where

$$a_{(k)}^{\beta} = \begin{bmatrix} a_{11}^{(k)\beta} & a_{12}^{(k)\beta} & a_{13}^{(k)\beta} & 0 & 0 & a_{16}^{(k)\beta} \\ a_{21}^{(k)\beta} & a_{22}^{(k)\beta} & a_{23}^{(k)\beta} & 0 & 0 & a_{26}^{(k)\beta} \\ a_{31}^{(k)\beta} & a_{32}^{(k)\beta} & a_{33}^{(k)\beta} & 0 & 0 & a_{36}^{(k)\beta} \\ 0 & 0 & 0 & a_{44}^{(k)\beta} & a_{45}^{(k)\beta} & 0 \\ 0 & 0 & 0 & a_{54}^{(k)\beta} & a_{55}^{(k)\beta} & 0 \\ a_{61}^{(k)\beta} & a_{62}^{(k)\beta} & a_{63}^{(k)\beta} & 0 & 0 & a_{66}^{(k)\beta} \end{bmatrix} \tag{7}$$

Matrix of stiffness coefficients k – rank of an anisotropic layer in the direction of the major coordinate lines α_1, α_2;

$$\sigma_{(k)} = [\sigma_{11}^{(k)}, \sigma_{22}^{(k)}, \sigma_{33}^{(k)}, \sigma_{23}^{(k)}, \sigma_{13}^{(k)}, \sigma_{12}^{(k)}]^T,$$
$$\varepsilon_{(k)} = [\varepsilon_{11}^{(k)}, \varepsilon_{22}^{(k)}, \varepsilon_{33}^{(k)}, \varepsilon_{23}^{(k)}, \varepsilon_{13}^{(k)}, \varepsilon_{12}^{(k)}]^T$$

– Column matrix of stress and strain layer in the direction of the major coordinate lines α_1, α_2. Matrix coefficients are expressed through the coefficients of the matrix $a_{(k)}$ with dependencies:

$$a_{11}^{(k)\beta} = a_{11}^{(k)} \cos^4 \beta_{(k)} + 2\left(a_{12}^{(k)} + 2a_{66}^{(k)}\right)\sin^2 \beta_{(k)} \cos^2 \beta_{(k)} + a_{22}^{(k)} \sin^4 \beta_{(k)},$$

$$a_{22}^{(k)\beta} = a_{11}^{(k)} \sin^4 \beta_{(k)} + 2\left(a_{12}^{(k)} + 2a_{66}^{(k)}\right)\sin^2 \beta_{(k)} \cos^2 \beta_{(k)} + a_{22}^{(k)} \cos^4 \beta_{(k)},$$

$$a_{12}^{(k)\beta} = \left[a_{11}^{(k)} + a_{22}^{(k)} - 2\left(a_{12}^{(k)} + 2a_{66}^{(k)}\right)\right]\sin^2 \beta_{(k)} \cos^2 \beta_{(k)} + a_{12}^{(k)},$$

$$a_{33}^{(k)\beta} = a_{33}^{(k)}, \quad a_{13}^{(k)\beta} = a_{13}^{(k)} \cos^2 \beta_{(k)} + a_{23}^{(k)} \sin^2 \beta_{(k)},$$
$$a_{23}^{(k)} = a_{13}^{(k)} \sin^2 \beta_{(k)} + a_{23}^{(k)} \cos^2 \beta_{(k)},$$
$$a_{44}^{(k)\beta} = a_{44}^{(k)} \cos^2 \beta_{(k)} + a_{55}^{(k)} \sin^2 \beta_{(k)},$$
$$a_{45}^{(k)\beta} = \left(a_{44}^{(k)} - a_{55}^{(k)}\right)\sin \beta_{(k)} \cos \beta_{(k)},$$

$$a_{55}^{(k)\beta} = a_{44}^{(k)} \sin^2 \beta_{(k)} + a_{55}^{(k)} \cos^2 \beta_{(k)},$$
$$a_{36}^{(k)\beta} = \left(a_{23}^{(k)} - a_{13}^{(k)}\right)\sin \beta_{(k)} \cos \beta_{(k)},$$
$$a_{66}^{(k)\beta} = \left[a_{11}^{(k)} + a_{22}^{(k)} - 2\left(a_{12}^{(k)} + 2a_{66}^{(k)}\right)\right]\sin^2 \beta_{(k)} \cos^2 \beta_{(k)} + a_{66}^{(k)},$$

$$a_{16}^{(k)\beta} = \left[a_{22}^{(k)} \sin^2 \beta_{(k)} - a_{11}^{(k)} \cos^2 \beta_{(k)} + \left(a_{12}^{(k)} + 2a_{66}^{(k)}\right)\left(\cos^2 \beta_{(k)} - \sin^2 \beta_{(k)}\right)\right]\sin \beta_{(k)} \cos \beta_{(k)},$$

$$a_{(k)\beta}^{26} = \left[a_{(k)}^{22} \cos^2 \beta_{(k)} - a_{(k)}^{11} \sin^2 \beta_{(k)} - \left(a_{(k)}^{12} + 2a_{(k)}^{66}\right)\left(\cos^2 \beta_{(k)} - \sin^2 \beta_{(k)}\right)\right]\sin \beta_{(k)} \cos \beta_{(k)},$$

For further presentation of the material system of equations (6) – (7) conveniently represented as:

$$\sigma_{(k)}{}^{\alpha} = a_{(k)\alpha}{}^{\beta} \varepsilon_{(k)}{}^{\alpha}, \qquad \sigma_{(k)}{}^{\alpha 3} = a_{(k)\alpha 3}{}^{\beta} \varepsilon_{(k)}{}^{\alpha 3} \tag{8}$$

Where in equation (8) introduced the following notation:

$$\sigma_{(k)}{}^{\alpha} = [\sigma_{11}^{(k)}, \sigma_{22}^{(k)}, \sigma_{33}^{(k)}, \sigma_{12}^{(k)}]^T, \qquad \sigma_{(k)}{}^{\alpha 3} = [\sigma_{23}^{(k)}, \sigma_{13}^{(k)}]^T,$$
$$\varepsilon_{(k)}{}^{\alpha} = [\varepsilon_{11}^{(k)}, \varepsilon_{22}^{(k)}, \varepsilon_{33}^{(k)}, \varepsilon_{12}^{(k)}]^T, \qquad \varepsilon_{(k)}{}^{\alpha 3} = [\varepsilon_{23}^{(k)}, \varepsilon_{13}^{(k)}]^T,$$

$$a_{(k)\alpha}{}^{\beta} = \begin{bmatrix} a_{11}^{(k)\beta} & a_{12}^{(k)\beta} & a_{13}^{(k)\beta} & a_{16}^{(k)\beta} \\ a_{21}^{(k)\beta} & a_{22}^{(k)\beta} & a_{23}^{(k)\beta} & a_{26}^{(k)\beta} \\ a_{31}^{(k)\beta} & a_{32}^{(k)\beta} & a_{33}^{(k)\beta} & a_{36}^{(k)\beta} \\ a_{61}^{(k)\beta} & a_{62}^{(k)\beta} & a_{63}^{(k)\beta} & a_{66}^{(k)\beta} \end{bmatrix},$$

$$a_{(k)\alpha 3}{}^{\beta} = \begin{bmatrix} a_{44}^{(k)\beta} & a_{45}^{(k)\beta} \\ a_{54}^{(k)\beta} & a_{55}^{(k)\beta} \end{bmatrix} \tag{9}$$

In the case where the composite is a set of n different oriented layers of unidirectional material contained elastic characteristics of the package layers are the obvious with relations:

$$\sigma^{\alpha} = a_{\alpha}^{\beta} \varepsilon^{\alpha}, \qquad \sigma^{\alpha 3} = a_{\alpha 3}^{\beta} \varepsilon^{\alpha 3}, \tag{10}$$

Where $a_{ij}^{\beta} = \sum_{k=1}^{n} a_{ij}^{(k)\beta} h_{(k)}', \quad h_{(k)}' = h_{(k)} / h$ – relative thickness of the k-rank layer.

The elastic constants of multilayer stack in tension can be obtained by transforming the system of equations (10) to mean

$$\sigma_{11} = a_{11}^{\beta} \varepsilon_{11} + a_{12}^{\beta} \varepsilon_{22} + a_{13}^{\beta} \varepsilon_{33} + a_{16}^{\beta} \varepsilon_{12},$$
$$0 = a_{21}^{\beta} \varepsilon_{11} + a_{22}^{\beta} \varepsilon_{22} + a_{23}^{\beta} \varepsilon_{33} + a_{26}^{\beta} \varepsilon_{12},$$
$$0 = a_{31}^{\beta} \varepsilon_{11} + a_{32}^{\beta} \varepsilon_{22} + a_{33}^{\beta} \varepsilon_{33} + a_{36}^{\beta} \varepsilon_{12}, \tag{11}$$
$$0 = a_{61}^{\beta} \varepsilon_{11} + a_{62}^{\beta} \varepsilon_{22} + a_{63}^{\beta} \varepsilon_{33} + a_{66}^{\beta} \varepsilon_{12}.$$

Substituting $E_1 = \dfrac{\sigma_{11}}{\varepsilon_{11}}$ in the first equation of the system of equations (11) and pre-expressing strain ε_{22}, ε_{33}, ε_{12} with assistance ε_{11} from the remaining (3-x) equations (11), it is easy to find the value E_1:

$$E_1 = \frac{\det a_\alpha^\beta}{M_{11}} \qquad (12)$$

Where M_{11} – minor element a_{11}^β of the matrix a_α^β. Similarly, there are other values of the constants:

$$E_2 = \frac{\det a_\alpha^\beta}{M_{22}}, \qquad E_3 = \frac{\det a_\alpha^\beta}{M_{33}} \text{ -} \qquad (13)$$

Young modulus;

$$G_{12} = \frac{\det a_\alpha^\beta}{M_{44}}, \qquad G_{13} = a_{55}^\beta - \frac{(a_{45}^\beta)^2}{a_{44}^\beta}, \qquad G_{23} = a_{44}^\beta - \frac{(a_{45}^\beta)^2}{a_{55}^\beta} \qquad (14)$$

Shear modulus;

$$v_{12} = \frac{M_{12}}{M_{11}}, \qquad v_{13} = \frac{M_{13}}{M_{11}}, \qquad v_{23} = \frac{M_{23}}{M_{22}} \text{ -} \qquad (15)$$

Poisson's ratios. The remaining three values of Poisson's ratio v_{21}, v_{31}, v_{32} re using the well-known relations

$$v_{ij} E_j = v_{ji} E_i \qquad (i, j = 1,2,3). \qquad (16)$$

Here, the first index of the Poisson coefficient indicated a direction of load application; the second one demonstrated a direction of the lateral deformation, which was induced by this force.

On the basis of the proposed algorithm, using an applied packet of PC MATHCAD 14 programs, we obtained numerical values of elastic characteristics of the reinforced material.

III. STRESSED STATE OF MULTI-LAYERED CYLINDERS UNDER ACTION OF INTERNAL PRESSURE.

In [7], a solution of a problem of a stress-deformed state of an anisotropic cylindrical shell of a finite length induced by an action of internal and external hydrostatic pressure for the case of state without moment was proposed to be solved similar to a solution of Lame problem for a thick-wall isotropic cylinder. Under an action of only internal pressure p, expressions for solution of lame problem for a thick-wall isotropic cylinder. Under an action of only internal pressure P, expressions for normal pressure tangents for a cylindrical coordinate system (Fig. 2) should be written as:

$$\sigma_r = -p r_1^{k+1} \left[1 - (\frac{\rho}{r_2})^{2k} \right] \left\{ \left[1 - (\frac{r_1}{r_2})^{2k} \right] \rho^{k+1} \right\}^{-1}, \qquad (17)$$

$$\sigma_\theta = p k r_1^{k+1} \left[1 + (\frac{\rho}{r_2})^{2k} \right] \left\{ \left[1 - (\frac{r_1}{r_2})^{2k} \right] \rho^{k+1} \right\}^{-1}, \qquad (18)$$

$$\sigma_z = -p r_1^{k+1} \left[(b_{13} + k b_{23} - g k b_{45}) \cdot (\frac{\rho}{r_2})^{2k} - (b_{13} - k b_{23} - g_{-k} b_{45}) \right] \times$$

$$\times \left\{ b_{33} \left[1 - (\frac{r_1}{r_2})^{2k} \right] \rho^{k+1} \right\}^{-1}, \qquad (19)$$

$$\sigma_{\theta z} = -p r_1^{k+1} \left[g_k (\frac{\rho}{r_2})^{2k} + g_{-k} \right] \left\{ \left[1 - (\frac{r_1}{r_2})^{2k} \right] \rho^{k+1} \right\}^{-1}, \qquad \sigma_{rz} = 0, \qquad (20)$$

Where $\sigma_r, \sigma_\theta, \sigma_z$ – normal stresses respectively in the radial, circumferential and longitudinal directions; $\sigma_{\theta z}, \sigma_{rz}$ – shear stresses in the circumferential and radial directions; r_1, r_2 – inner and outer radii of the cylinder; $r_1 \leq \rho \leq r_2$ – coordinate of the cylinder; b_{ij} $(i, j = 1, 2, \ldots, 6)$ – coefficients compliance matrix reinforced material and that are associated with coefficients stiffness matrices (10) relations

$$b_\alpha^\beta = (a_\alpha^\beta)^{-1}, \qquad b_{\alpha 3}^\beta = (a_{\alpha 3}^\beta)^{-1}.$$

In addition, in (17) - (20) introduces additional notation:

$$k = \sqrt{\frac{\beta_{33}}{\beta_{22}}}; \qquad g_k = \frac{\beta_{16} + k \beta_{26}}{\beta_{66}}; \qquad g_{-k} = \frac{\beta_{16} - k \beta_{26}}{\beta_{66}};$$

$$\beta_{ij} = b_{ij} - \frac{b_{i3} b_{j3}}{b_{33}} \qquad (i, j = 1, 2, \ldots, 6). \qquad (21)$$

Dependences (17) to (21) were derived taking into account an assumption that an elastic symmetry, which was perpendicular to a normal to a middle cylinder surface, was present in every point of the cylinder. In this case of anisotropy, under an action of a normal pressure, the thick-wall cylinder will not only change the curvature radii of transversal cross-sections but also change the initial length and be whirled.

Employing formulas (17) to (21), to derive the values of maximal and minimal stresses taking place at points of the internal and external surfaces of the considered cylinder seems to be not complicated ($\rho = r_1$, $\rho = r_2$). We should like to note that calculating the stressed state of anisotropic cylindrical shells employing the formulas (17) to (21), theoretical result for thin-walled cylinders could be derived with a practically assumed accuracy($r_1/r_2 \geq 0,8$). In this case, the indicated dependences do not allow one to determine changes of the cylinder stressed state induced by a presence of material inter-phase structure defects and an influence of conditions of ends fixation.
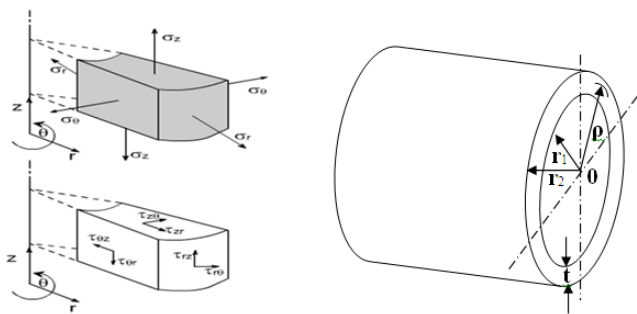
Figure 2 Design scheme of the pipe in a cylindrical coordinate system

IV. MATERIALS PROPERTIES

A fiber is a material made into a long filament. According to [5], a single fiber usually has a diameter up to 15 um. Bigger diameters generally increase the probability of surface defects. The aspect ratio of length and diameter can be ranging from thousand to infinity in continuous fibers. They usually occupy 30-70% of the volume of the composite and 50% of its weight.

The main functions of fibers are to carry the load and provide stiffness, strength, thermal stability and other structural properties to the FRP [2]. To perform these functions, the fibers in FRP composite must have high modulus of elasticity, high ultimate strength, low variation of strength among fibers, high stability of their strength during handling and high uniformity of diameter and surface dimension among fibers.

Basically, the properties of FRP reinforced composites depend on the properties of its components, their volume ratio, the orientation of the fibers in the matrix and properties of the fiber-matrix bond [8].

The type of fibers used as the reinforcement is the basics for classification of FRP composites. There are three types of fibers dominating civil engineering industry: glass, carbon and aramid fibers. The table below presents properties of various kinds of fibers. Econcret = 30 GPa, υconcret = 0.43 number of fiber glass layers 21 . Properties of glass, aramid and carbon fibers (Table.1), Comparison of properties of various construction materials to FRP composites (Table.2).

TABLE 1 PROPERTIES OF GLASS, ARAMID AND CARBON FIBERS [5]

Typical properties	Fiber glass aramid carbon					
	Glass		Aramid		Carbon	
	E- Glass	S- Glass	Kevlar 29	Kevlar 49	HS [high strength]	HM[high modulus]
Density ρ [g/cm³]	2.6	2.5	1.44	1.44	1.8	0.19
Youngrs Modulus E [GPa]	72	87	100	124	230	370
Tensile strength R [MPa]	1.72	2.53	2.27	2.27	2.48	1.79
Extension [%]	2.4	2.9	2.8	1.8	11	0.5

TABLE 2 COMPARISON OF PROPERTIES OF VARIOUS CONSTRUCTION MATERIALS TO FRP COMPOSITES [5]

Typical properties	Material					
	Duralumin	Titan TiA 16V a4	Steel St52	GFRP	GFRP quasiisotr. vol. Fraction 60%	GFRP orthotropic vol. Fraction 60%
Density ρ [g/cm³]	2.8	4.5	7.8	2.1	1.5	1.7
Tensile strength Rm [MPa]	350	800	510	720	900	3400
Specific strength Rm/ρ [Mpa.cm³/g]	125	178	65	340	600	2000
Youngrs Modulus E [GPa]	75	11	210	30	88	235
Specific Youngrs Modulus E/ρ	27	2	27	14	59	138

V. RESULTS AND DISSECTION

On the basis of the presented calculation models and techniques, which were developed for calculation of such class of problems, the stressed state of the concrete and steel cylinder, which had the internal surface radius $r_1 = 0.9\,м$, was studied. The shell was fabricated by reeling up a single-directed glass strip. As a whole, such cylindrical shell was composed of 2 single-directed layers. The reeling angle of every layer was determined using a code of material structure. Totally, 10 versions of the shell reinforcing were considered (Table.3).

TABLE 3 THE STRUCTURE OF THE LAMINATE PIPE.

NO.	Code
1	[0_{10}°/0^{-}°]$_S$
2	[0° / 30°/0° / 30°/0° / 30°/0° / 30°/0° / 30°/0^{-}°]$_S$
3	[0° / 45°/0° / 45°/0° / 45°/0° / 45°/0° / 45°/0^{-}°]$_S$
4	[0° / 60°/0° / 60°/0° / 60°/0° / 60°/0° / 60°/0^{-}°]$_S$
5	[0° / 75°/0° / 75°/0° / 75°/0° / 75°/0° /75°/0^{-}°]$_S$
6	[0° / 90°/0° / 90°/0° / 90°/0° / 90°/0° / 90°/0^{-}°]$_S$
7	[0° / ±30°/0° / ±45°/0° / ±60°/02° /0^{-}°]$_S$
8	[0_2° / ±30°/0° / 0_2°/ ±60°/0_2° /0^{-}°]$_S$
9	[0_2° / ±45°/0° / 0_2°/ ±90°/0_2° /0^{-}°]$_S$
10	[0° / 15°/0° / 30°/0° /45°/0° / 60°/0° / 75°/0^{-}°]$_S$

Thickness layer is $\delta = 1.9\ mm$ the other characteristics of the monolayer components are carbon earlier.

For any given structure of concrete and steel were found physical and mechanical characteristics as a composite material with one plane of elastic symmetry (Table 4). In this Cartesian coordinate system (Fig. 1) is replaced by a cylindrical (Fig. 2).

TABLE 4 THE ELASTIC CONSTANTS OF FIBER AND CONCRETE.

№ Code	E_z, MPa	E_θ, MPa	E_r, MPa	$G_{\theta z}$, MPa	G_{zr}, MPa	$G_{\theta r}$, MPa	$\nu_{z\theta}$	ν_{zr}	$\nu_{\theta r}$	$\nu_{\theta z}$	ν_{rz}	$\nu_{r\theta}$
1	152200	112400	112200	35770	36860	23780	0.5	0.43	0.43	0.43	0.31	0.43
2	139700	111000	112300	28720	35020	25130	0.5	0.41	0.41	0.47	0.33	0.42
3	133700	113600	112400	39760	33390	26610	0.5	0.4	0.41	0.49	0.34	0.4
4	132500	120600	112600	38660	31930	28230	0.5	0.41	0.41	0.49	0.35	0.39
5	134400	129400	112700	36680	30970	29510	0.5	0.43	0.43	0.49	0.36	0.38
6	135700	133700	112700	35770	30630	30010	0.49	0.44	0.44	0.49	0.37	0.37
7	132300	115900	112600	40210	33120	27520	0.5	0.4	0.41	0.5	0.34	0.39
8	19800	115700	112500	38430	34370	26270	0.5	0.41	0.42	0.47	0.33	0.41
9	138700	121800	112600	37550	33120	27520	0.5	0.42	0.42	0.48	0.34	0.39
10	138100	117600	112500	38180	33550	26730	0.5	0.42	0.42	0.48	0.34	0.4

Values of normal and tangential stresses at points of the internal and external cylinder surface under internal pressure intensity $q = 40\,MPa$ are presented in (Table. 5) Analysis of results demonstrated that a changed code did not practically influence the values of normal stresses in a circle direction σ_θ. In this case, an essential change of stress values $\sigma_{\theta z}$ of a transversal shear $\sigma_{\theta z}$ and normal axial stresses σ_z took place.

Studies, which were performed for a stressed state of multi-layered shell having [02° / ±45°/0° / 02°/ ±90°/02° /0⁻°]S code, when the layer thickness was successively increased till a given value (Fig. 3 – 5), are of interest. As a whole, the shell thickness was determined by an expression $h = r_2 - r_1$. The value r_2 shown in Fig. 3 – 5, a value of the shell internal surface did not change and was equal to $r_1 = 0{,}9\,m$. Elastic constants for the presented set of layers did not depend on the shell thickness.

TABLE 5 STRESS STATE OF THICKNESS CYLINDER (H = 40 MM)

№ Code	$\rho = r_1$				$\rho = r_2$			
	σ_r, MPa	σ_θ, MPa	σ_z, MPa	$\sigma_{\theta z}$, MPa	σ_r, MPa	σ_θ, MPa	σ_z, MPa	$\sigma_{\theta z}$, MPa
1	-40	928	-287	0	0	880	-725	38.3
2	-40	929	-287	37	0	879	-734	21.5
3	-40	929	-298	1.5	0	879	-743	0
4	-40	929	-292	-5	0	879	-752	7.9
5	-40	929	-298	-12.4	0	879	-759	0
6	-40	929	-273	0	0	879	-761	0
7	-40	930	-282	0	0	879	-746	47.9
8	-40	930	-305	0	0	879	-739	30.2
9	-40	930	-292	0	0	879	-747	0
10	-40	930	-288	14	0	879	-743	0
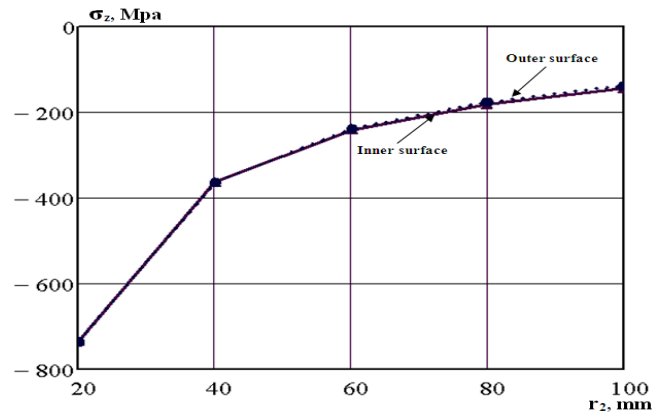
Figure 3 Relation between stress σ_z and thickness of the pipe

Figure 4 Relation between stress $\sigma_{\theta z}$ and thickness of the pipe
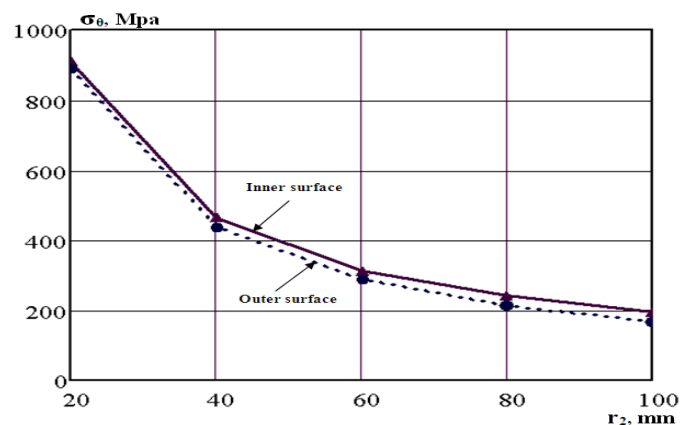
Figure 5 Relation between stress σ_θ and thickness of the pipe

We should like to note that the increased shell thickness did not practically change a difference of normal stresses σ_θ in the circle direction at points of the internal and external surfaces. So, for example, if the shell thickness was $r_2 - r_1 = h = 40\,мм$, this difference was 35MPa, if it was

$r_2 - r_1 = h = 80 мм$, the difference was 45MPa. Analyzing dependences of σ_z stresses on the shell thickness, one could notice that in anisotropic shells, when r/h>20, essentially high stress values σ_z arose. Such stresses could be a reason for destruction of the binder in a considered reinforced material. In this case, conditions for an ideal contact between the layers, which were considered in a continuous-structure theory of anisotropic plates and shells turned out to be essentially violated.

VI. CONCLUSIONS

The paper proposed a method for determining the elastic constants of anisotropic material, which consists of a set of reinforced layers. Reviewed ten variants of multilayer anisotropic hollow cylinders with different structure reinforcement. For each variant of reinforcement to determine the stress state of the cylinder under the action of internal pressure. It is shown that with increasing thickness of the membrane normal stress in direction θ (σθ) increase but normal stress in direction z (σz) decreases.

VII. SUMMARY

The analysis of separate layers reinforced by high-module fibers on the macro level elastic properties definition methods is offered. In the case when a composite is a set of layers with different re-enforcement directions, methodology of determination the reduced elastic properties over all layers in package in tote is offered. The deflected mode of multi-layered hollow cylinder with the different variants of re-enforcement of its separate layers under internal pressure is analyzed.

REFERENCE

[1]   L. C. Bank, Composites for Construction - Structural Design with FRP Materials, John Wiley & Sons, Inc., 2006 ., pp. 1-19

[2]   C. Tuakta, Use of Fiber Reinforced Polymer Composite in Bridge Structures, Massachusetts Institute of Technology, 2005., pp. 50

[3]   T. Keller, Use of Fibre Reinforced Polymers in Bridge Construction, IABSE Structural Engineering Documents No 7. 2003., pp. 319-331

[4]   R. Lopez-Anido, T. Naik, Emerging Materials for Civil Infrastructure. State of the Art, American Society of Civil Engineers, 2000., pp. 232

[5]   H. Zobel, Mosty kompozytowe, 50. Jubileuszowa Konferencja Naukowa KILiW PAN i KN PZITB, Krynica, 2004., p. 93

[6]   S.M. Vereshchaka, For discrete-structural theory of multilayer shells with structural defects / / Bulletin of NTU "KPI". Collection of scientific papers. Special Issue: Dynamics and strength of machines. - Kharkov: NTU "KPI". - 2004. - № 31. - S. 39 - 46.

[7]   S.G. Lekhnitskii, The theory of elasticity of an anisotropic body. - Moscow: Nauka, 1977. – pp. 416.

[8]   G.A. , Jara Estudio de la aplicabilidad de materiales compuestos al diseno de estructuras de contencion de tierras y su interaccion con el terreno, para su empleo en obras de infraestructura viaria - Tesis doctoral, Universidad Politecnica de Madrid, E.T.S. de Ingenieros de Caminos, Canales y Puertos, Departamento de Ingenieria y Morfologia del Terreno, Madrid 2008., p. 426.